American Mineralogist, Volume 85, pages 495–508, 2000

Solubility and stability of zeolites in aqueous solution: II. Calcic clinoptilolite and mordenite

LIANE G. BENNING,* RICHARD T. WILKIN,† AND HUBERT L. BARNES

Department of Geosciences, Pennsylvania State University, University Park, Pennsylvania 16802, U.S.A.

ABSTRACT

The solubilities of Ca-exchanged clinoptilolite (Cpt-Ca) and Ca-exchanged mordenite (Mor-Ca) have been measured in aqueous solutions between 25 and 275 °C and at saturated water vapor pressures. Natural zeolites were cation exchanged to close to Ca end-member composition (90% for Cpt-Ca, and 98% for Mor-Ca). The controlling dissolution reactions may be written as:

$$\text{Cpt-Ca: } Ca_{0.56}(Al_{1.12}Si_{4.88}O_{12})(3.9H_2O) + 8.1H_2O = 0.56Ca^{2+} + 1.12Al(OH)_4^- + 4.88Si(OH)_{4(aq)}^0$$

$$\text{Mor-Ca: } Ca_{0.515}(Al_{1.03}Si_{4.97}O_{12})(3.1H_2O) + 8.9H_2O = 0.515Ca^{2+} + 1.03Al(OH)_4^- + 4.97Si(OH)_{4(aq)}^0$$

These reactions are reversible as shown by equilibrium constants calculated for approach from under- and supersaturation. The log K_{sp} for Cpt-Ca increases from –26.9 at 25 °C to a maximum of –16.9 at 275 °C, whereas for Mor-Ca the equilibrium constant varies from –25.3 at 25 °C to –17.7 at 265 °C. The solubilities for both zeolites increase with increasing temperature showing a positive enthalpy for the dissolution reaction. At lower temperatures Cpt-Ca is slightly more soluble than Mor-Ca, which agrees with natural observations where mordenite and clinoptilolite commonly occur together spatially but mordenite is in general the higher-temperature phase. A comparison with other exchanged clinoptilolites indicates that Cpt-Ca is more stable than the Na, K, and Mg varieties. The results demonstrate that the exchanged cation has a large effect on the solubility behavior, and that divalently exchanged varieties are less soluble than monovalent varieties. From the solubility constants, the standard Gibbs free energies of formation for hydrous Cpt-Ca and Mor-Ca at 25 °C and 1 bar were determined to be –6387 ± 5 kJ/mol and –6275 ± 7 kJ/mol respectively. However, compared to the hydration states and the aluminosilicate structure, the effect of the cation on the Gibbs free energies of formation is small.

INTRODUCTION

The occurrences of natural zeolites are restricted to the low temperature (~3–400 °C), low pressure (~0.001–3 kbar) environments of the "zeolite facies," which was defined as the transitional facies between diagenesis and metamorphism (Fyfe et al. 1958; Coombs et al. 1959; Zen 1961; Hay 1978). In the zeolite-water system, dissolution and precipitation as well as adsorption and exchange reactions govern cation fixation. The need to understand these processes has become even more pertinent because zeolites have been recognized as major components of the tuffs at the Nevada Test Site. Zeolites (clinoptilolite, mordenite, and analcime, in particular) are potential absorbers for several components of high-level radioactive waste in the proposed repository at Yucca Mountain (Nevada, U.S.A.) (e.g., Smyth 1982; Ogard et al. 1984; Bish 1984; Pabalan 1994; Carey and Bish 1996; Bertetti et al. 1996; Kastenberg and Gratton 1997). However, the conditions under which such processes occur are not well known because thermodynamic and kinetic data for the zeolite-water system are still scarce.

In natural samples, the main cation in clinoptilolite (Cpt) is typically Na^+; however, Ca^{2+}, K^+, and Mg^{2+} are also present (see untreated Cpt in Table 1). The amount of water in the crystal structure of zeolites is one of the main factors influencing their stability, i.e., Gibbs free energy of formation (Carey and Bish 1996, 1997; Wilkin et al. 1997; Wilkin and Barnes 1999). This is particularly true for Ca-rich zeolites (Coombs et al. 1997, 1998), because they absorb more water than zeolites rich in other cations (Deer et al. 1985; Armbruster 1993). In this study, the experimental material is referred to as clinoptilolite, in accordance with the original description of the Castle Creek zeolite by Mondale et al. (1988) and Sheppard (1991). In addition, this agrees with the established criteria for distinguishing between clinoptilolite and its isostructural form heulandite (Si/Al ratio, Ca and water content; Mason and Sand 1960; Mumpton 1960; Alietti 1972; Boles 1972; Armbruster 1993; Hey and Bannister 1934; Valueva 1995; Table 1). In this study, 90 mol% exchange was achieved for the Cpt-Ca, but only 80 mol% ex-

* Present address: School of Earth Sciences, University of Leeds, Leeds LS2 9JT, U.K; E-mail: liane@earth.leeds.ac.uk
† Present address: U.S. Environmental Protection Agency, National Risk Management Research Laboratory, Ada, OK 74820.

TABLE 1. Chemical composition, structural formula, and calcium molar ratios of clinoptilolite and mordenite samples used in this study

	Castle Creek clinoptilolite untreated	Castle Creek clinoptilolite Ca-exchanged (n = 2)	Poona mordenite untreated (n = 3)	Poona mordenite Ca-exchanged
SiO_2	65.50	64.0	68.6	67.9
TiO_2	0.08	0.11	<0.01	<0.02
Al_2O_3	12.40	12.5	11.8	11.9
Fe_2O_3	0.48	0.78	0.08	0.03
MgO	1.07	0.32	0.02	0.01
CaO	0.72	6.34	3.74	6.50
MnO	<0.01	<0.01	<0.01	<0.02
Na_2O	3.57	0.10	2.86	0.10
K_2O	2.34	0.28	0.03	0.06
LOI	12.90	15.3	13.0	12.80
Total	99.06	99.6	100.13	99.10
Ca end-member	5 mol%	90 mol%	53 mol%	98 mol%
		Formula proportions based on 12 O atoms		
Si	4.91	4.88	4.99	4.97
Al	1.09	1.12	1.01	1.03
Mg	0.12	0.04	0.00	0.00
Ca	0.06	0.52	0.29	0.515
Na	0.52	0.01	0.40	0.01
K	0.21	0.03	0.00	0.00
H_2O	3.22	3.89	3.17	3.13
Si/Al	4.50	4.35	4.93	4.83
Ca/(Ca+Na)	0.19	0.99	0.59	0.99
Ca/(Ca+K)	0.36	0.97	1	1
Ca/(Ca+Mg)	0.33	0.96	1	1

Note: LOI = loss of ignition, for solids equilibrated at 50% relative humidity.
Castle Creek Clinoptilolite: initial = $Na_{0.52}K_{0.21}Ca_{0.06}Mg_{0.12}(Al_{1.08}Si_{4.91}O_{12})(3.22H_2O)$.
Cpt-Ca = $Ca_{0.56}(Al_{1.12}Si_{4.88}O_{12})(3.89H_2O)$.
Poona Mordenite: initial = $Na_{0.40}Ca_{0.29}(Al_{1.01}Si_{4.99}O_{12})(3.17H_2O)$.
Mor-Ca = $Ca_{0.515}Al_{1.03}Si_{4.97}O_{12})(3.13H_2O)$.

change for Cpt-Mg (Benning, unpublished data). This result is consistent with the observation that Mg^{2+} is located in a water-rich, octahedrally coordinated, low-occupancy site (Koyama and Takeuchi 1977). Mordenite (Mor) is one of the most silica-rich zeolites, having an Si/Al ratio close to 5. The main cations are Na^+ and Ca^{2+}, usually in nearly equal amounts, whereas K^+ and Mg^{2+} are minor constituents (Passaglia 1975; Passaglia et al. 1995; untreated Mor in Table 1). Following the exchange experiments, a fairly pure (98 mol%) Ca end-member was obtained (Table 1); however, an Mg end-member of the Poona mordenite could not be attained (maximum 53 mol% exchange, Benning; unpublished data).

The relative stability relations of clinoptilolite and mordenite, as well as their transformation to higher-temperature phases such as analcime/wairakite or feldspar (depending on the predominant cation), have been studied extensively. Natural observations have been reported by Ueda et al. (1980) and Tsitsishvili et al. (1992), for example, whereas Hawkins (1967), Boles (1971), Hawkins et al. (1978), Ueda et al. (1980), and Kusakabe et al. (1981) have carried out experimental studies. Clinoptilolite forms in nature primarily from intermediate-silica-content glasses at temperatures between 20 and 80 °C (Iijima 1982) and decomposes at 70–120 °C (Iijima 1982; Bish 1984). In experiments, clinoptilolite synthesis depends on the starting materials (e.g., glass, gel, or solution), pH, temperature, and solution composition. The transformation to analcime occurs mainly in alkaline, high-salt solutions at 100–300 °C (Ames and Sand 1958; Koizumi and Roy 1960; Boles 1972; Abe and Aoki 1976; Hawkins et al. 1978; Kusakabe et al. 1981; Ilin and Voloshinets 1985; Wilkin and Barnes 1998b). Mordenite, on the other hand, is more commonly an alteration product of silica-rich glasses (Harris and Brindley 1954; Coombs et al. 1959; Wirsching 1975), forming also in mostly alkaline, high-salt solution at 70–150 °C. However, its stability can be as high as 250–400 °C, and the reactions from clinoptilolite via mordenite to analcime span an even larger (100–400 °C) temperature range (Ames and Sand 1958; Combs et al. 1959; Iijima 1974; Abe and Aoki 1975; Wirsching 1975; Ueda et al. 1980; Kusakabe et al. 1981). In nature, clinoptilolite and mordenite commonly occur together, and both natural observations and experimental evidence suggest that clinoptilolite and mordenite form at about the same temperatures and under similar chemical conditions, but paragenetic textures indicate that mordenite is predominant at the higher temperatures.

Despite their importance and the wide variety of environments in which zeolites occur (Mumpton 1978; Tsitsishvili et al. 1992; Tschernich 1992; and references therein), as well as the extensive studies done on the zeolite-water system, it is surprising that the solubilities of clinoptilolite and mordenite in aqueous solutions have not been studied until recently (Murphy et al. 1996; Wilkin and Barnes 1998a). In addition, the relative stabilities of clinoptilolite, mordenite, and their high-temperature counterparts are still equivocal. Equilibrium constants derived from solubility measurements are fundamental for the understanding of cation exchange and alumina- and silica-release capacities of zeolites in natural environments. To model the behavior of zeolites in such settings, it is necessary to understand the effects of mono- and divalent cations on the solubility of the alumino-silicate framework. Wilkin and Barnes (1998a) have presented the first solubility measurements on

analcime, and Na- and K-exchanged clinoptilolite from 25 to 300 °C. However, the solubility of zeolites with divalent cations has not been studied. The aim of this study, therefore, has been to determine the solubility of Ca-exchanged clinoptilolite (Cpt-Ca) and mordenite (Mor-Ca) at 25–275 °C at saturated water-vapor pressures. The derived equilibrium constants are used to extract Gibbs free energies of formation, and to examine the relative stability relations of the Ca-, Na-, K-, and Mg-exchanged varieties of clinoptilolite with respect to mordenite and analcime/wairakite.

EXPERIMENTAL METHODS

The experimental methods are similar to those of the first paper of this series (Wilkin and Barnes 1998a). Here we present a summary and details of some changes in methodology.

Treatment, exchange and characterization

Exceptionally high purity (>95%) natural clinoptilolite and mordenite were used in the solubility experiments. For clinoptilolite, the same starting material as described in Wilkin and Barnes (1998a) was used (Castle Creek, Idaho, U.S.A.). The crystals have a platy morphology, generally <5–10 μm in size, and form aggregates of ~50–100 μm. The mordenite (kindly provided by H. S. Pandalai, Indian Institute of Technology, Bombay, India) stems from an altered tholeiitic basalt near Poona (Maharashtra, India; Sukheswala et al. 1972, 1974; Passaglia 1975). The mordenite forms needle-like crystals up to 200 μm, which also become aggregated after cleaning and exchange. The bulk clinoptilolite and mordenite samples were crushed and powdered in an agate mortar, sieved and hand-picked for visible impurities, and then purified by gravitational settling in deionized water.

Standard materials for solubility measurements were produced by treatment with 8 *m* $CaCl_2$ solution (Fisher reagent grade). Initially, clinoptilolite was exchanged for 32–55 days in closed, regularly shaken plastic bottles at 50 °C. The supernatant solutions were changed every second day; however, this procedure provided only ~76 mol% exchange. Therefore, for both clinoptilolite and mordenite, higher-temperature exchange experiments were performed in teflon vials (25 mL) with a mixture of ~ 20 mL of $CaCl_2$ solution and 1–3 g of zeolite. The vials were placed in a hydrothermal autoclave using water as the confining pressure medium. The autoclave was heated to 120 °C and kept in continuous rocking mode for 20–40 days, except when the solutions in the vials were changed (~20 times). The resulting solids were washed thoroughly with doubly distilled, deionized water and then analyzed (Table 1) showing a maximum exchange of 90.0 mol% for Cpt-Ca and 97.9 mol% for Mor-Ca. This treatment changed the Si/Al ratios of the initial clinoptilolite from 4.48 ± 0.04 to a final value of 4.35 ± 0.10 . The change in Si/Al ratio is the result of selective dissolution of silica during the exchange experiments (losing ~30 ppm/exchange). Nevertheless, the X-ray diffraction (XRD) pattern of the final Ca-exchanged variety still corresponds to clinoptilolite. For mordenite, the change in Si/Al ratio is less pronounced because the cation exchange was less extensive.

The cation-exchanged zeolites were characterized by XRD using a Rigaku Geigerflex and by scanning electron microscopy (SEM) using a JEOL SX-20A instrument. Major-element concentrations were determined by inductively coupled, plasma atomic emission spectroscopy (Leeman PS3000, ICP-AES; $2\sigma = 3–5\%$), and the water content of samples equilibrated at 50% relative humidity was determined by weight loss after ignition (LOI) at 900 °C. The chemical composition, stoichiometries, and the calculated, idealized chemical formulas are tabulated in Table 1.

Solubility experiments

Due to temperature restrictions two different methods were used for the solubility measurements. The high-temperature solubility measurements were carried out in large volume autoclaves placed in a rocking furnace (Barnes 1971). About 300–400 mL of freshly boiled, doubly distilled, oxygen- and CO_2-free water, cooled under a constant flow of oxygen-free N_2, was transferred under a nitrogen atmosphere to an autoclave with 10–15 g of the cleaned and exchanged zeolite. The autoclave was sealed, placed in the furnace, and heated to the desired temperature. The temperature (±1.5 °C) was measured with a chromel-alumel thermocouple inserted through the closure of the autoclave to contact the solution. During the experiments the autoclave was rocked so that solution and solids were constantly mixed and temperature gradients in the autoclave were reduced to a minimum. All experiments were conducted at saturated water-vapor pressures. After several days the rocker was stopped and the solids were allowed to settle. Subsequently, approximately 10 mL of solution was collected at the experimental temperature and pressure by using a syringe attached to a valve assembly. The samples were immediately filtered through a 0.2 μm, cellulose acetate filter (Valuprep), diluted with 3% HNO_3, and the total concentrations of Si, Al, Na, K, Ca, and Mg were analyzed by ICP-AES. To minimize equilibration with atmospheric CO_2, quench pH was measured at room temperature with a micro combination electrode (Corning) within 1 min after sample collection; the high-temperature pH values were calculated using the computer code SOLMINEQ.88 (Kharaka et al. 1988). The composition and morphology of the solids after the runs were characterized with ICP-AES, XRD, and SEM techniques. The formation of new phases was not observed under saturated water-vapor pressure and a maximum temperature of 275 °C. This is in accordance with Wilkin and Barnes (1998a), who showed that quartz precipitates in experiments with Na-clinoptilolite and water at temperatures as high as 300 °C.

Experiments below 100 °C and at 1 bar were carried out with Cpt-Ca and Mor-Ca as well as with the Na- and K-exchanged varieties of Castle Creek clinoptilolite (Cpt-Na, Cpt-K) and with a sedimentary analcime (Wik) (Wilkin and Barnes 1998a, 1998b) for intervals up to ~13 months. The latter were used as control experiments, although, in contrast to Wilkin and Barnes (1998b), a pH buffer was not used and longer equilibration times were achieved (Appendix 1). Slow reaction rates at T <100 °C constrained these experiments to approach equilibrium from undersaturation only. About 1–3 g of solids were mixed with 50–75 mL of double-distilled water in 125 mL plastic bottles and kept in an oven (50 ± 2 °C) or on the bench top (23 ± 5 °C) for long time periods. Homogeneous mixing was ensured by regularly shaking the bottles. Sample preparation and measurements were equivalent to the higher-temperature runs described above.

RESULTS

Equilibrium, reversibility, and temperature dependence

Equilibrium was indicated when solution compositions remained constant over time and proven by reversibility, i.e., demonstrated by ramping temperature up and down and achieving the same solubility from both under- and supersaturation. Note, however, that the experiments at 25 and 50 °C were approached only from undersaturation. Although new phases were not identified, it is possible that the observed incongruent dissolution behavior is a result of the formation of subordinate quantities of Al-rich silicates that precipitated and re-dissolved during the high-temperature runs. It is assumed, however, that such phases would act as buffers for the activities of aqueous silica and alumina. The progress of two experiments with Cpt-Ca and Mor-Ca between 100 and 275 °C and at saturated water-vapor pressure is shown in Figures 1a and 1b. The monovalent cations as well as silica and alumina attain, within the uncertainties of the measurements, the same equilibrium values when approached from undersaturation as well as supersaturation. The total aqueous Ca concentrations are reversible but vary inversely with temperature. In the Cpt-Ca (run c3, Fig. 1a) when equilibrium is approached from supersaturation the values for calcium at 175 °C are somewhat higher than at approach from undersaturation. This disparity is interpreted to reflect slower attainment of equilibrium when approached from supersaturation. However, the effect on the final equilibrium constants is negligible (Fig. 2). Mor-Ca shows the same variation but better agreement between approach from under- and supersaturation (Fig. 1b). The decrease in aqueous Ca^{2+} concentration with increasing temperature is in accordance with the higher stability of calcium-rich clinoptilolites and mordenites in comparison with the other cation-exchanged varieties (see below).

Below 100 °C, equilibrium was only approached from undersaturation and the uncertainties in the calculated equilibrium constants are large (Appendix 1). Several experiments were performed at 25 and 50 °C with Na- and K-exchanged varieties of Castle Creek clinoptilolite and with an analcime sample from Wikieup (Na-x, K-x, and Wik in Appendix 1). These experiments were conducted for time intervals up to 9500 hours long. However, when comparing the individual equilibration times and solubilities with the data of Wilkin and Barnes (1998a), a discrepancy is apparent. Wilkin and Barnes (1998a) conducted experiments at higher pH and for shorter equilibration times (<4000 h). Their solubilities are lower than those measured in the longer-term experiments in this study (Appendix 1). This discrepancy is not easily explained because similar conditions and methods were employed. The reasons can be multiple; the most-important ones are non-reversibility of the reactions, time constraints, evaporation rates, uncertainties in Si and Al speciation, pH variations, and homogenization rates.

Equilibrium constants and data treatment

If the chemical compositions of natural clinoptilolite and mordenite are normalized to the same number of oxygen atoms (in this study, 12), the end-members are very similar in structural formula. This fact allows similar treatment of the solubility data. For the temperature and pH range of the experiments in this study (25 to 275 °C and $pH_{25\,°C}$ = 6.1–8.8),

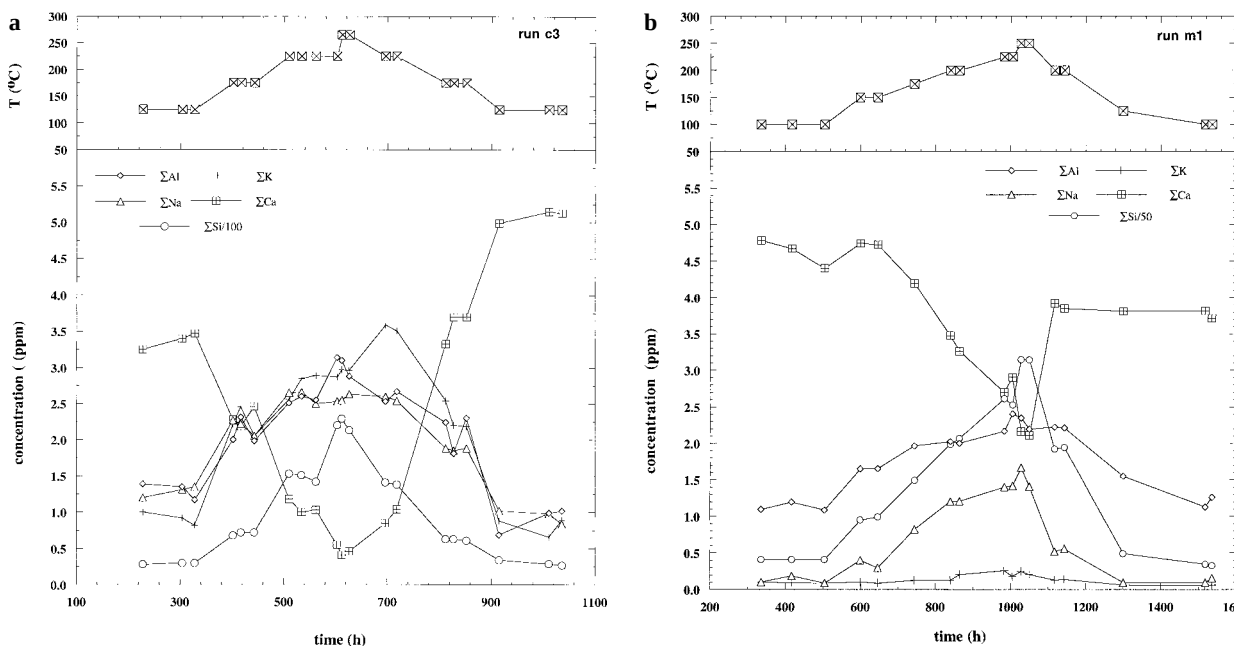

FIGURE 1. Concentration-time-temperature diagram showing attainment of equilibrium and reversibility of the solubility reactions in experiments with (**a**) Cpt-Ca and (**b**) Mor-Ca (data in Appendix 1). The bottom Y-axis shows concentration of Al, Si, Ca, Na, and K, normalized to fit on the same diagram, whereas the top part represents the variation in temperature.

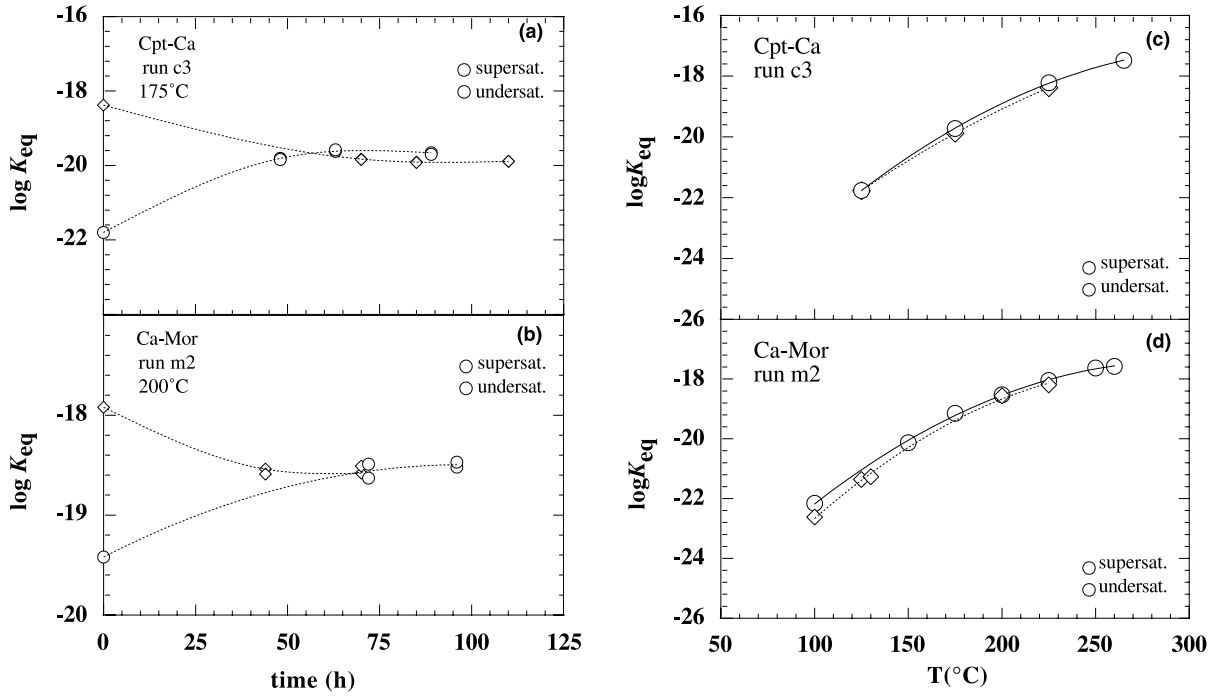

FIGURE 2. Variation of the equilibrium constants with time at (**a**) 175 °C for Cpt-Ca and (**b**) at 200 °C for Mor-Ca; and with temperature (**c**) for Cpt-Ca and (**d**) for Mor-Ca. The lines represent best-fit lines through all points. The size of the symbols corresponds to the maximum variation in equilibrium constant.

the dominant aqueous Si and Al species are $Si(OH)_4^0$ (Busey and Mesmer 1977; Johnson et al. 1992) and $Al(OH)_4^-$, respectively (Wesolowski 1992; Castet et al. 1993; Bourcier et al. 1993; Wesolowski and Palmer 1994). Following Wesolowski and Palmer (1994) it is assumed that the concentration of the neutral species $Al(OH)_3^0$ is insignificant at low temperatures. At high temperatures, the calculated pH_T values are always above neutrality where the assumption that $Al(OH)_4^-$ is the only significant species is valid and the correction for $Al(OH)_3^0$ is negligible (Castet et al. 1993; Wesolowski and Palmer 1994; see also Appendix 2).

The reactions describing the equilibria involved in the dissolution of the Ca-exchanged varieties of clinoptilolite and mordenite may be written as:

$$Ca_{0.56}(Al_{1.12}Si_{4.88}O_{12})(3.9H_2O)_{Cpt\text{-}Ca} + 8.1H_2O_{(l)} = 0.56Ca^{2+} + 1.12Al(OH)_4^- + 4.88Si(OH)_4^0 \quad (1)$$

$$Ca_{0.515}(Al_{1.03}Si_{4.97}O_{12})(3.1H_2O)_{Mor\text{-}Ca} + 8.9H_2O_{(l)} = 0.515Ca^{2+} + 1.03Al(OH)_4^- + 4.97Si(OH)_4^0 \quad (2)$$

For the end-member compositions shown in Table 1, unit activities for the solids are postulated. This standard-state convention is consistent with the progressive dehydration of clinoptilolite that occurs along the boiling curve of pure water as temperature increases (e.g., Wilkin and Barnes 1999). The standard state of the aqueous species is the ideal 1 molal solution with $a_{H_2O} = 1.0$. Note that the standard state of the zeolites implies that, independent of temperature, the ion activity product (Q), which at equilibrium is equal to the equilibrium constant (K_{eq}), can be calculated for example for Cpt-Ca from:

$$K_{eq,Cpt\text{-}Ca} = a_{Ca^{2+}}^{0.56} \cdot a_{[Al(OH)_4^-]}^{1.12} \cdot a_{[Si(OH)_4^0]}^{4.88} \quad (3)$$

Note that at $a_{H_2O} = 1.0$, the calculation of the equilibrium constants is independent of the zeolite hydration state. The Ca-rich varieties of clinoptilolite and mordenite used in this study were close to end-member compositions (Table 1), and the concentrations of Na^+, K^+, and Mg^{2+} in the exchanged solids were low. Therefore, the assumption of end-member composition with unit activity and negligible influence of minor cations on the solubility product is reasonable. This assumption also is corroborated by the fact that the equivalent ratios of Ca^{2+} with respect to Na^+, K^+, and Mg^{2+} are close or equal to 1 (Table 1). Therefore, in order to satisfy charge-balance requirements, total Ca^{2+} has been set equal to the stoichiometric proportion of Al. The individual aqueous ion-activity coefficients were calculated by means of the extended Debye-Hückle equation (Helgeson 1969; Helgeson and Kirkham 1974) using the B˙ deviation function. The values for the ion-size parameters corresponding to the distance of closest approach have been taken from Kieland (1937) and the activity coefficient for the neutral $Si(OH)_4^0$ species was taken as 1. The ionic strength in all experimental aqueous solutions was below 10^{-3} and, consequently, the activity corrections are small. Appendix 1 contains the individual equilibrium constants together with data on time interval, direction of approach to equilibrium, temperature, $pH_{25\,°C}$, and solution composition.

The values and sources for the equilibrium constants used in the calculations are summarized in Appendix 2.

Equilibrium solubility and reversibility of the reactions for both zeolites was also demonstrated using calculated equilibrium constants. When approaching equilibrium from undersaturation or supersaturation, within the limits of the analytical and experimental uncertainties, the same equilibrium constant values were achieved (Fig. 2). It is important to note that the equilibrium constants plotted in Figure 2 and tabulated in Appendix 1 were calculated assuming that Ca is the only cation in the lattice of the zeolites. To test whether the minor cations in the lattice, i.e., Na^+, K^+, and Mg^{2+}, have an effect on the overall solubility constants, "mixed" log K_{eq} were calculated taking into consideration the minor cations. However, the variation in equilibrium constant values is smaller than the combined experimental and analytical uncertainties. For example, for run c3 (Appendix 1) the equilibrium constant at 175 °C is –19.82 ± 0.14 when calculated with Ca set equal to the stoichiometric proportion of Al, whereas the same equilibrium constant is –19.94 ± 0.10 when calculated taking into consideration Na, K, and Mg. The same can be shown for Mor-Ca, where the percentage of other cations in the lattice is far smaller. This agreement demonstrates that as long as the solids have close to end-member composition, minor cations in the zeolite lattice have little to no effect on the solubility behavior. Therefore, the assumption that sufficiently pure end-member compositions were achieved during the exchange experiments is warranted. However, as will be shown later, these minor cations, and especially the hydration state and the Si/Al ratios, have a large effect on the Gibbs free energy of formation. From the averaged values of log K of the individual samples at each temperature, the steady-state equilibrium constants for both Cpt-Ca and Mor-Ca were calculated and are tabulated in Table 2 together with the standard deviations.

DISCUSSION

Reaction thermodynamics

Solubility constants derived from experimental work provide a useful basis for the derivation of thermodynamic properties at any given pressure and temperature. However, in this study the experiments were conducted along the liquid/vapor curve and only temperature-dependent equations for Cpt-Ca and Mor-Ca were derived. The molar Gibbs free energy of reaction (ΔG_r^0) has been calculated at each temperature directly from the equilibrium constants in Table 2 using the dependence $\Delta G_r^0 = -2.303RT\log K_T$, with T in Kelvin. In order to calculate other thermodynamic functions, the equilibrium constants for reaction 1 and 2 were regressed to a temperature-dependent equation of the form:

$$\log K_T = a + bT + c/T + d\log T \quad (4)$$

with T in Kelvin. The values of the regression coefficients are given in the following equations and the fitted curves are plotted together with the experimental data in Figures 3a (Cpt-Ca) and 3b (Mor-Ca).

$$\log K_{\text{Cpt-Ca}} = -170.214 - 0.025T - 5.624/T + 60.988\log T \quad (5)$$

$$\log K_{\text{Mor-Ca}} = -348.22 - 0.107T - 170.581/T + 142.023\log T \quad (6)$$

For Cpt-Ca and Mor-Ca, the regressed values are in close agreement with the experimental data. The largest discrepancy is obvious at low temperatures for Mor-Ca. Note, however, that for Mor-Ca: (1) only few data were available at 25 °C (Appendix 1), (2) no data were available at 50 °C, and (3) shorter equilibration times were achieved. Therefore, the fitting of the equilibrium constants for Mor-Ca was done relying solely on the high-temperature data and the few 25 °C data were omitted in the fitting procedure (Eq. 6). For Cpt-Ca, however, the regression included the low temperature data. The log K values calculated at 25 °C for Cpt-Ca using Equation 5 deviate from the measured values by a maximum of 0.25 log units (which lies well within the analytical and experimental uncertainties) but by more than 1.5 log units for Mor-Ca. The regressions based only on the reversed high-temperature data are used in the subsequent calculations and in the comparisons with literature data. However, for clinoptilolite, it could be shown that a fit of all data (including the 25 and 50 °C data points) is in very close agreement with the experimental data (i.e., the deviation at T >25 °C is less that 0.25 log units, Fig. 3).

The thermodynamic functions have been calculated from the partial derivatives of Equations 5 and 6 with respect to temperature at constant pressure. The first derivative provides the enthalpy change, ΔH_r^0, whereas the entropy change (ΔS_r^0) was calculated in the conventional way (see Table 3). The equations and the values of the thermodynamic properties for Cpt-Ca and Mor-Ca at 25–275 °C and saturated water-vapor pressures are listed in Table 3.

TABLE 2. Equilibrium constants for the dissolution of Ca clinoptilolite and Ca mordenite, pertaining to reactions 1 and 2 from 25 to 275 °C and at saturated water-vapor pressure

T (°C)	log $K_{\text{Cpt-Ca}}$	log $K_{\text{Mor-Ca}}$
25*	–26.92 ± 0.56	–25.32 ± 0.13†
50*	–25.03 ± 0.22	
100	–	–22.31 ± 0.21
125	–21.80 ± 0.12	–21.36 ± 0.38
130	–	–21.27 ± 0.05
150	–	–20.32 ± 0.19
175	–19.74 ± 0.13	–19.42 ± 0.20
200	–	–18.54 ± 0.05
225	–18.15 ± 0.17	–18.08 ± 0.09
250	–	–17.92 ± 0.38
260	–	–17.58 ± 0.04
265	–17.33 ± 0.33	–17.71 ± 0.14
275	–16.96 ± 0.01	

Note: The tabulated values represent the average over all samples at each temperature (Appendix 1).
* Pressure is 1 bar.
†Value not used in fitting procedure (Eq. 6).

Comparison with previous work

Solubility data for natural zeolites are scarce. Murphy et al. (1996) and Wilkin and Barnes (1998a) have published the only solubility data available for clinoptilolite while no direct solubility measurements for mordenite have been published. For clinoptilolite at 25 °C, Murphy et al. (1996) estimated log K_{eq} to be –25.5 for an idealized Na end-member with an Si/Al ratio of 5. However, differences in primary cation and Si/Al ratio make a comparison with the equilibrium constant for Cpt-Ca

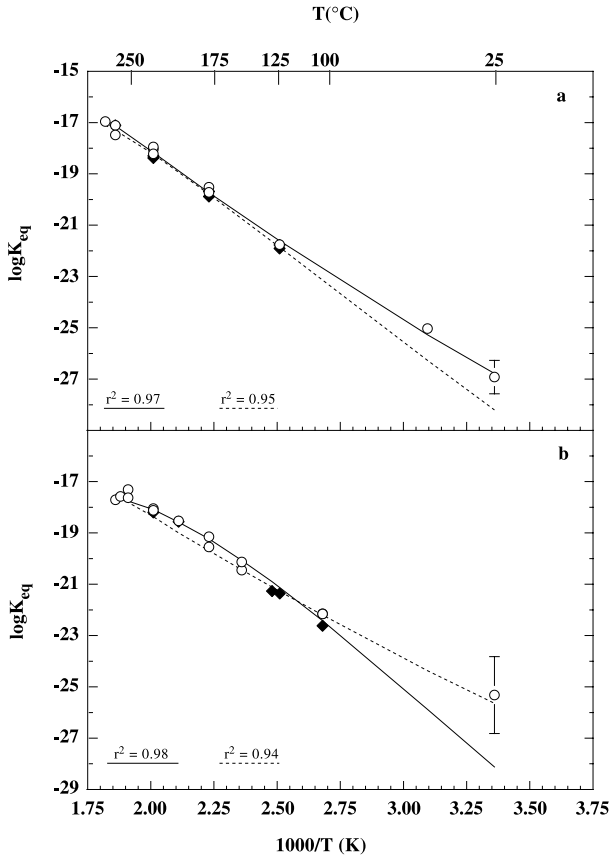

FIGURE 3. Experimental equilibrium constants plotted as a function of reciprocal temperature for (**a**) Cpt-Ca and (**b**) Mor-Ca. The symbols represent the experimentally derived equilibrium constants; open symbols = approach from undersaturation; filled symbol = approach from supersaturation. The solid curves represent the fitted Equations 5 and 6; the dotted curves represent in (**a**) a fit excluding the T < 100 °C data, whereas in (**b**) the 25 °C data were included.

TABLE 3. Thermodynamic properties for Ca-CPT (reaction # 1) and Ca-MOR (reaction # 2) calculated using the coefficients from equations (4) and (5) and the equations listed below

	Cpt-Ca			Mor-Ca		
T (°C)	ΔG_r^0	ΔH_r^0	ΔS_r^0	ΔG_r^0	ΔH_r^0	ΔS_r^0
25	152.9 ± 3.2	108.7	–148	160.5 ± 14.3	167	21
50	156.4 ± 1.48	114.0	–131	160.1 ± 12.4	164	13
100	162.2 ± 2.5	122.7	–106	160.2 ± 1.1	152	–22
125	164.7 ± 0.9	126.1	–97	161.1 ± 2.3	142	–48
150	167.1 ± 1.2	129.0	–90	162.6 ± 2.0	130	–78
175	169.3 ± 1.1	131.2	–85	165.0 ± 0.9	114	–116
200	171.3 ± 1.8	132.9	–81	168.3 ± 1.8	97	–151
225	173.3 ± 1.6	133.9	–79	172.6 ± 1.4	77	–193
250	175.3 ± 2.5	134.4	–78	177.9 ± 1.5	54	–237
275	179.5 ± 2.1	134.2	–83	184.5 ± 1.6	28	–285

Notes: $\Delta G_r^0 = -2.303RT\log K_{Cpt/Mor}$.
$\Delta H_r^0 = 2.303R(bT^2\text{-}c+dT/2.303)$.
$\Delta S_r^0 = (\Delta H_r^0 - \Delta G_r^0) / T$.
T in Kelvin, ΔG_r^0 and ΔH_r^0 in kJ/mol and ΔS_r^0 in J/(mol·K).

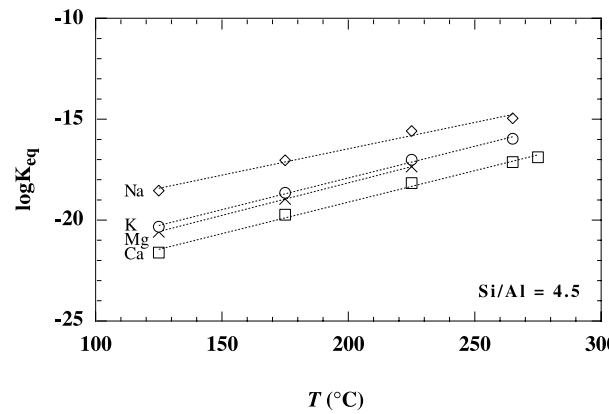

FIGURE 4. Equilibrium constants for Ca-, Mg- Na-, and K-exchanged Castle Creek clinoptilolite from this study and from the literature. Note that in all log K calculations, the activity of water is equal to 1. The data for Na- and K-exchanged clinoptilolite are from Wilkin and Barnes (1998a) and the data for Mg-exchanged clinoptilolite are from Benning et al. (1997) and Benning (unpublished data).

from the present study difficult. Wilkin and Barnes (1998a) measured the solubility of the Na- and K-exchanged Castle Creek clinoptilolite between 25 and 265 °C and at liquid water-vapor pressures. Their data, together with preliminary equilibrium constants for the Mg-variety of the Castle Creek clinoptilolite (Benning et al. 1997; Benning, unpublished data), can be compared with the results from this study (all exchanged varieties have an Si/Al ratio equal, or close, to 4.5). However, note that water contents vary significantly among the various cation-exchanged forms (see Table 1). In Figure 4, a trend of increasing solubility at constant temperature is apparent from mono- to divalent clinoptilolites. These results perhaps can be correlated with observations on natural and synthetic Ca-rich clinoptilolites, which have been shown to persist longer at higher temperatures compared to their Na counterparts (Coombs et al. 1959; Wirsching 1981; Bowers and Burns 1990). In addition, the transformation of Ca-rich clinoptilolite to its high-temperature equivalent—wairakite—is also documented at much higher temperature than the transformation of the Na-rich clinoptilolite to its high-temperature counterpart—analcime (Wirsching 1981; Browne et al. 1989; Wilkin and Barnes 1998b).

The standard Gibbs free energies of formation, ΔG_f^0, for cation-exchanged hydrous and anhydrous clinoptilolite were calculated at 25 °C by combining the experimentally derived equilibrium constants with literature data for the Gibbs free energies of the aqueous species (cations, aluminum, silica, and water) by applying:

$$\Delta G^o_{f,Cpt} = x\Delta G^0_{f,cat} + x\Delta G^0_{f,Al(OH)_4^-} + y\Delta G^0_{f,Si(OH)_4^0} - (n+m)\Delta G^0_{f,H_2O} - \Delta G^0_{r,Cpt} \quad (7)$$

with x, y, n, and m being the stoichiometric coefficients from Equation 1 and the Gibbs free energies are taken from Table 3 and from the literature (Table 4). Note that the calculations for clinoptilolite are based on 50% relative humidity. For hydrous Cpt-Ca at 25 °C, a ΔG_f^0 value of –6387 ± 5 kJ/mol has been calculated.

From previous measurements on ideal Na, K, and Mg end-member clinoptilolite (Murphy et al. 1996; Wilkin and Barnes 1998a; Benning et al. 1997) and mixed-cation clinoptilolites (Hemingway and Robie 1984; Johnson et al. 1991), the Gibbs

TABLE 4. Gibbs free energies of formation (kJ/mol) of aqueous species at 25 °C

Species	Na^+	K^+	Ca^{2+}	Mg^{2+}	$Al(OH)_4^-$	$Si(OH)_4^0$	$H_2O_{(l)}$
ΔG_f^0	–261.9[1]	–280.0[1]	–554.0[1]	–455.0[1]	–1306.1[2]	–1307.8[3]	–237.2[4]

Note: (1) Tanger and Helgeson (1988); (2) Bourcier et al. (1993) and Diakonov et al. (1996); (3) Walther and Helgeson (1977); (4) Helgeson and Kirkham (1974).

TABLE 5. Compositions and standard state Gibbs free energies of formation for hydrous clinoptilolites from this study and the literature in a comparison (see text)

Source and main cation*	Ca mol%	Na mol%	K mol%	Mg mol%	Si/Al	H_2O mol%	ΔG_f^0 kJ/mol
1 Cpt-Na	0	100	0	0	5	4	–6355
2 Cpt-Ca-Mg	42.7	7.7	13.7	35.9	4.35	3.67	–6319
3 Cpt-Ca-Na	46.3	29.6	16.7	7.4	4.21	3.67	–6359
4 Cpt-Na	0.9	95.5	2.2	1.4	4.50	3.5	–6268
4 Cpt-K	0.8	1.2	97.0	1.0	4.50	2.7	–6107
5 Cpt-Ca	90.0	6.3	1.3	2.4	4.35	3.9	–6387†/–6395
6 Cpt-Mg	7.7	6.6	6.7	78.9	4.47	3.8	–6287†/–6301
7 Cpt-Na							–6274‡
7 Cpt-K							–6117‡
7 Cpt-Ca							–6397‡

* 1 = Murphy et al. (1996); 2 = Hemingway and Robie (1984) and Bowers and Burns (1990); 3 = Johnson et al. (1991); 4 = Wilkin and Barnes (1998a); 5 = this study; 6 = Benning et al. (1997); 7 = La Iglesia and Aznar (1986).
† Calculated with major cation set equal to the stoichiometric proportion of Al, whereas second value included the minor cations in the calculation of the log *K* and ΔG_f^0 Note that the minor cations change the ΔG_f^0 by a maximum 8–14 kJ/mol. The largest change is obseved for Cpt-Mg, which is in accordance with low exchange extent of this material (79 mol% Mg).
‡ Calculated assuming the same hydration state, Si/Al ratios, and cation content apply as in sources 4 and 5.

free energies of formation for 25 °C and 1 bar were derived. However, the variable Si/Al ratios and water contents as well as different mixed-cation compositions render comparisons equivocal (Table 5). For example, Hemingway and Robie (1984) used a Ca- and Mg-rich clinoptilolite with Si/Al = 4.35 and H_2O = 3.67 from which a ΔG_f^0 = –6319 kJ/mol was calculated (Bowers and Burns 1990). Johnson et al. (1991) studied a Ca-Na clinoptilolite with Si/Al = 4.21 and H_2O = 3.6 and derived ΔG_f^0 = –6359.5 kJ/mol. For Cpt-Na, a comparison between ΔG_f^0 = –6355 kJ/mol (after Murphy et al. 1996) and ΔG_f^0 = –6267.9 kJ/mol (Wilkin and Barnes 1998a) shows that a difference of more than 1 log unit in equilibrium constants accounts for a change in ΔG_f^0 of only 5–10 kJ/mol. Larger changes, up to 85 kJ/mol, arise from the differences in Si/Al (Si/Al = 4.5 vs. 5.0) and hydration states (H_2O = 3.5 vs. 4.0). In the present study, the calculations of the Gibbs free energy of formation for clinoptilolite are based on 50% relative humidity, and the Ca-exchanged clinoptilolite from this study (Table 1) contains 15.3 wt% water. However, the hydration state may in fact increase at 100% relative humidity. Following Carey and Bish (1996), the maximum expected increase in water content is 0.7 wt%. As a result, the hydration state potentially may increase by about 0.15, resulting in a more negative $\Delta G_{f,\,298,1bar}^0$ by about 36 kJ/mol.

A direct comparison of clinoptilolite stability (Gibbs free energies of formation, ΔG_f^0) can be made only with the Na-, K-, Mg-, and Ca-exchanged varieties of the Castle Creek clinoptilolite (Wilkin and Barnes 1998a; Benning et al. 1997; Benning, unpublished data and this study), as all have Si/Al = 4.5. The ΔG_f^0 for the anhydrous and hydrous forms of Na-, K-, Mg-, and Cpt-Ca, and the theoretical values calculated after La Iglesia and Aznar (1986) for the hydrous forms of these cation-exchanged clinoptilolites, are tabulated in Table 5 and plotted in Figure 5. Note that the Gibbs free energies of formation for the Ca and Mg varieties listed in Table 5 were calculated including the free energy contribution of the minor cations. However, the contribution is a maximum of 8–14 kJ/mol (e.g., for Cpt-Ca –6387 kJ/mol vs. –6395 kJ/mol), which indicates that the minor cations in the lattice of the zeolite framework have only a small contribution toward the Gibbs free energy of formation. It is apparent that with decreasing degree of exchange (i.e., Cpt-K > Cpt-Na > Cpt-Ca > Cpt-Mg), the differences in measured and calculated Gibbs free energy become larger. However, from Figure 5 it can be concluded that at fixed Si/Al ratios the contribution of the exchangeable cation on the Gibbs free energy of formation is relatively small (<30 kJ/mol), and the dominant parameter is the hydration state. This is in accordance

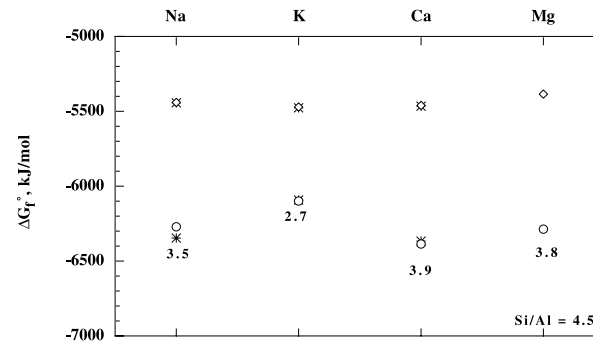

FIGURE 5. Gibbs free energies of formation for hydrous (circles) and anhydrous (diamonds) Na-, K-, Mg-, and Ca-exchanged clinoptilolite at 25 °C; stars and crosses are calculated after La Iglesia and Aznar (1986). Note that, following La Iglesia and Aznar (1986), the Gibbs free energies of formation for hydrous clinoptilolites were calculated assuming that the Gibbs free energies of H_2O in clinoptilolite are the same as that in liquid water. The numbers under the symbols for the hydrous Gibbs free energies represent the water content in the structure of each exchanged variety of clinoptilolite determined by LOI (Na and K from Wilkin and Barnes 1998a; Mg from Benning et al. 1997; Ca, see Table 1).

with studies on the thermodynamics of hydration for clinoptilolite from low-temperature calorimetric and thermogravimetric measurements (Johnson et al. 1991; Carey and Bish 1996, 1997) and hydrothermal data (Wilkin et al. 1997). In addition, in Figure 5 it is obvious that the calculated values after La Iglesia and Aznar (1986) are in good agreement with the experimental values from this study. Note, however, that the main reason for this agreement lies in the fact that the calculations after La Iglesia and Aznar (1986) also rely strongly on the chemical composition of the experimental solid used in the solubility studies (Table 1).

For mordenite, the high-temperature equilibrium constants derived in the current study were used to extrapolate to 25 °C, 1 bar ($\log K_{\text{Mor-Ca}} = -28.12$) and to calculate a corresponding ΔG_f^0 Mor-Ca of –6275 kJ/mol. The only other thermodynamic data available are those of Johnson et al. (1992), who performed calorimetric measurements on a CaNa- and Si-rich zeolite from Gobble (Oregon, U.S.A.), obtaining ΔG_f^0 Mor-Ca = –6248 kJ/mol. The difference of only ~27 kJ/mol between the data of Johnson et al. (1992) and this study can be explained due to differences in Ca content (61.5 vs. 98 mol%), Si/Al ratio (5.38 vs. 4.83), and H_2O content ($H_2O_{\text{Cpt-Ca-Na}} = 3.47$ vs. $H_2O_{\text{Cpt-Ca}} = 3.13$).

Systematic studies of variable cation content and variable Si/Al ratio in pure end-member compositions of mordenite, as well as exact determinations of the hydration states of clinoptilolite and mordenite at hydrothermal temperatures, are necessary before a satisfactory model can be derived for the clinoptilolite and mordenite solid solutions.

Applications and conclusions

In experimental as well as equilibrium calculation studies, the major factors controlling the transformation of clinoptilolite to mordenite and analcime are primarily alkalinity and temperature (Hawkins 1967, 1978; Boles 1971; Abe and Aoki 1976; Bowers and Burns 1990; Wilkin and Barnes 1998b). The results of the present experimental study corroborate an earlier modeling study (Chipera and Bish 1997), showing that an additional parameter—the cation content—is an important factor.

The stability relations of the various exchanged clinoptilolite end-members, used in this study, can be represented in a diagram showing the temperature dependence of the ion-exchange Gibbs free energies (ΔG_{ex}^0) of Ca-Na and Na-K clinoptilolite (Fig. 6). The Gibbs free energy of exchange (ΔG_{ex}^0), is given by $-RT\ln K_{ex}$, where the exchange equilibria for Na-K and Ca-Na clinoptilolite are defined as $\log K_{ex(\text{Na-K})} = \log K_{\text{Cpt-Na}} - \log K_{\text{Cpt-K}}$ and $\log K_{ex(\text{Ca-Na})} = \log K_{\text{Cpt-Na}} - 0.5\log K_{\text{Cpt-Ca}}$, respectively. Their values are tabulated in Table 6 and were calculated as follows: $\Delta G^0_{ex(\text{Na-K})} = -RT/\nu\cdot[2.303(\log K_{\text{Cpt-Na}} - \log K_{\text{Cpt-K}})]$ for the Na-K exchange and $\Delta G^0_{ex(\text{Na-Ca})} = -RT/\nu\cdot[2.303(\log K_{\text{Cpt-Na}} - \log K_{\text{Cpt-Ca}})]$ for the Na-Ca exchange, with ν representing the stoichiometric coefficient for Na. Although the cumulative errors in ion-exchange parameters deduced from solubility constants are large (~1 log unit), it can be seen that Ca exchange is favored at temperatures above 50 °C, which is consistent with natural observations. Within the uncertainty levels, the data from this study agree well with the low-temperature data of Pabalan (1994), who obtained ion-exchange parameters via an approach that coupled a Margules model for solid solutions and the Pitzer model for aqueous activity coefficients (Fig. 6 and Table 6).

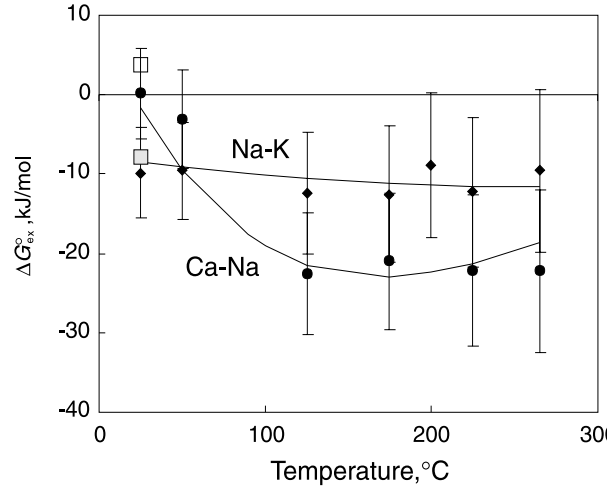

Figure 6. Temperature dependence of Gibbs free energies of exchange for Ca-Na and Na-K clinoptilolites. The symbols represent the experimental values whereas the fitted curves represent the values calculated from regression analyses. The circles are values for Cpt-Ca (Eq. 5, this study), diamonds are data for Na- and Cpt-K from Table 4 in Wilkin and Barnes (1998a), and the squares are data at 25 °C from Pabalan (1994) (open square, Ca-Na; shaded square, Na-K).

Table 6. Ion-exchange Gibbs free energies for Cpt-Na-, Cpt-K, and Cpt-Ca at 25 °C

Exchanged cations (source)	ΔG_{ex}^0 kJ/mol
Ca-Na (1)	4.19 ± 0.20
Na-K (1)	–7.98 ± 0.08
Ca-Na (2)	1.59 ± 5.70
Na-K (2 and 3)	–8.52 ± 5.70

Note: (1) Pabalan (1994); (2) this study; (3) Wilkin and Barnes (1998a).

In aqueous solution, the main factors governing the reactive behavior of Ca and Na end-member clinoptilolites are the activity of silica and the Ca/Na ratios (Fig. 7). The aqueous silica activity, although an important parameter, does not solely control the clinoptilolite-to-analcime reaction. Between 25 and 225 °C, and at any given silica activity, clinoptilolite is stabilized relative to analcime when the activity of the Ca-component within the clinoptilolite solid solution (or the aqueous Ca/Na ratio) is increased.

Relative to mordenite, clinoptilolite is stable at lower aqueous silica activities (Fig. 8). The mordenite field is characterized by a moderate Ca/H activity ratio and by amorphous silica saturation, whereas quartz saturation lies within the clinoptilolite field. For clinoptilolites with higher Si/Al ratios than mordenite, the stability relations between the two phases would switch, because their solubility behavior with temperature is very similar. Note, however, that in most natural samples, the Si/Al ratio in mordenite is higher than that in clinoptilolite (Tschernich 1992, and references therein). With respect to calcite saturation, at any given temperature, Ca-rich zeolites precipitate from unbuffered solutions, and from solution with low P_{CO_2}.

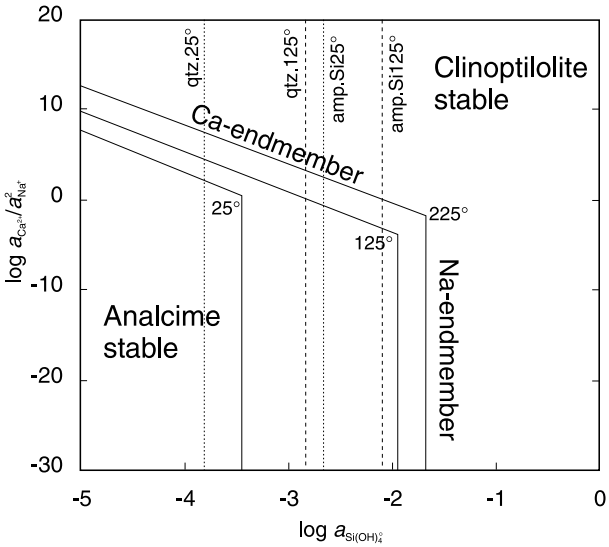

FIGURE 7. Stability relations between analcime and clinoptilolite from 25 to 225 °C calculated using data from this study and from Wilkin and Barnes (1998a). Quartz (qtz) and amorphous silica (amp. Si) data are from Rimstidt and Barnes (1980).

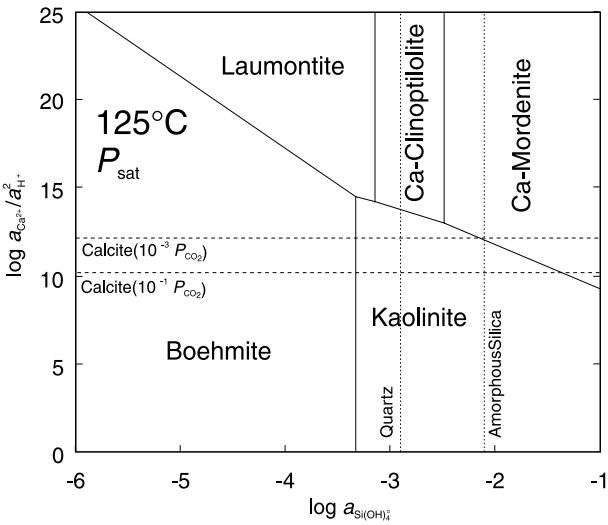

FIGURE 8. Stability diagram for the Ca zeolites laumontite, clinoptilolite, and mordenite at 125 °C as a function of silica activity and $a_{Ca^{2+}}/a^2_{H^+}$ ratio. Data for Cpt-Ca and Mor-Ca-this study; boehmite-Castet et al. (1993); kaolinite-Devidal et al. (1996); laumontite-Helgeson et al. (1978). The calculations are conducted for Cpt-Ca and Mor-Ca with Si/Al ratios of 4.5 and 4.8, whereas the other phases are assumed to have stoichiometric compositions. Note that at higher P_{H_2O}, wairakite would replace laumontite (Liou 1970).

On the other hand, the formation of laumontite—$CaAl_2Si_4O_{12}\cdot 4H_2O$—(and at higher temperatures and P_{H_2O} wairakite—$CaAl_2Si_4O_{12}\cdot 2H_2O$; Liou 1970) is favored by lower Si activities.

ACKNOWLEDGMENTS

The funding provided by the Swiss National Science Foundation for L.G.B. and by the Office of Basic Energy Sciences of the U.S. Department of Energy (DE-FG02-96ER14634) for R.T.W. is greatly appreciated. We gratefully acknowledge Henry Gong for analytical support throughout this study. We thank B. Carey, P. Neuhoff, S. Yang, and A. Navrotsky for their thorough review of this manuscript, which is much improved in this revised form.

REFERENCES CITED

Abe, H. and Aoki, M. (1975) Experiments on the interaction between Na_2CO_3-$NaHCO_3$ solution and clinoptilolite tuff, with reference to analcimization around Kuroko-type mineral deposits. Chemical Geology, 17, 89–100.

——(1976) Experiments on the hydrothermal alteration of mordenite rocks in sodium carbonate solution, with reference to analcimization around Kuroko deposits. Economic Geology, 70, 770–780.

Alietti, A. (1972) Polymorphism and crystal-chemistry of heulandites and clinoptilolites. American Mineralogist, 57, 1448–1462.

Ames, L.L. and Sand, L.B. (1958) Hydrothermal synthesis of wairakite and calcium-mordenite. American Mineralogist, 43, 476–480.

Armbruster, T. (1993) Dehydration mechanism of clinoptilolite and heulandite: single-crystal X-ray study of Na-poor, Ca-, K-, Mg-rich clinoptilolite at 100 K. American Mineralogist, 78, 260–264.

Barnes, H.L. (1971) Investigations on hydrothermal sulfide systems. In G.C. Ulmer, Ed., Research Techniques for High Pressure and High Temperatures, p. 317–355. Springer Verlag, New York.

Benning, L.G., Wilkin, R.T., and Barnes, H.L. (1997) The solubility of Ca- and Mg-clinoptilolite. V.M. Goldschmidt Conference, 1997, Program and Abstracts, 25.

Bertetti, F.P., Pabalan, R.T., Turner, D.R., and Almendares, M.G. (1996) Neptunium(V) sorption behavior in clinoptilolite, quartz and montmorillonite. Material Research Society Symposium Proceedings, 412, 631–638.

Bish, D.L. (1984) Effects of exchangeable cation composition on the thermal expansion/contraction of clinoptilolite. Clays and Clay Minerals, 32, 444–452.

Boles, J.R. (1971) Synthesis of analcime from natural heulandite and clinoptilolite. American Mineralogist, 56, 1724–1734.

——(1972) Composition, optical properties, cell dimensions, and thermal stability of some heulandite group zeolites. American Mineralogist, 57, 1463–1493.

Bowers, T.S. and Burns, R.G. (1990) Activity diagrams for clinoptilolite: Susceptibility of this zeolite to further diagenetic reactions. American Mineralogist, 75, 601–619.

Bourcier, W.L., Knauss, K.G., and Jackson, J.K. (1993) Aluminum hydrolysis constants to 250 °C from boehmite solubility experiments. Geochimica et Cosmochimica Acta, 57, 747–752.

Browne, P.R.L., Courtney, S.F., and Wood, C.P. (1989) Formation rate of calc-silicate minerals deposited inside drillhole casing, Ngatamariki geothermal field, New Zealand. American Mineralogist, 74, 759–763.

Busey, R.H. and Mesmer, R.E. (1977) Ionisation equilibria of silicic acid and polysilicate formation in aqueous sodium chloride solution to 300 °C. Inorganic Chemistry, 16, 2444–2450.

Carey, J.W. and Bish, D.L. (1996) Equilibrium in the clinoptilolite-H_2O system. American Mineralogist, 81, 952–962.

——(1997) Calorimetric measurement of the enthalpy of hydration of clinoptilolite. Clay and Clay Minerals, 45, 826–833.

Castet, S., Dandurant, J., Schott, J., and Gout, R. (1993) Boehmite solubility and aqueous aluminum speciation in hydrothermal solutions (90–350 °C): Experimental study and modeling. Geochimica et Cosmochimica Acta, 57, 4869–4884.

Chipera, S.J. and Bish, D.L. (1997) Equilibrium modeling of clinoptilolite-analcime equilibria at Yucca Mountain, Nevada, USA. Clay and Clay Minerals, 45/2, 226–239.

Coombs, D.S., Ellis, A.J., Fyfe, W.S., and Taylor, A.M. (1959) The zeolite facies, with comments on the interpretation of hydrothermal syntheses. Geochimica et Cosmochimica Acta, 17, 54–107.

Coombs, D.S., Alberti, A., Armbruster, T., Artioli, G., Colella, C., Galli, E., Grice, J.D., Liebau, F., Mandarino, J.A., Minato, H., Nickel, E.H., Passaglia, E., Peacor, D.R., Quartieri, S., Rinaldi, R., Ross, M., Sheppard, R.A., Tillmanns, E., and Vezzalini, G. (1997) Recommended nomenclature for zeolite minerals: report of the subcommittee on zeolites of the international mineralogical association, commission of new minerals and mineral names. The Canadian Mineralogist, 35, 1571–1606.

Coombs, D.S., Alberti, A., Armbruster, T., Artioli, G., Colella, C., Galli, E., Grice, J.D., Liebau, F., Mandarino, J.A., Minato, H., Nickel, E.H., Passaglia, E., Peacor, D.R., Quartieri, S., Rinaldi, R., Ross, M., Sheppard, R.A., Tillmanns, E., and Vezzalini, G. (1998) Recommended nomenclature for zeolite minerals: report of the subcommittee on zeolites of the international mineralogical association, commission of new minerals and mineral names. American Mineralogist, 83, 935 (abstract); website http://www.minsocam.org/MSA/AmMin/AmMineral.html.

Deer, W.A., Howie, R.A., and Zussman, J. (1985) An introduction to the rock-forming minerals. Longman Group Limited, Essex.

Devidal, J.L., Dandurand, J.L., and Gout, R. (1996) Gibbs free energy of formation

of kaolinite from solubility measurement in basic solution between 60 and 170 °C. Geochimica et Cosmochimica Acta, 60, 553–564.
Diakonov, I., Pokrovsky, G., Schott, J., Castet, S., and Gout, R. (1996) An experimental and computational study of sodium-aluminum complexing in crustal fluids. Geochimica et Cosmochimica Acta, 60, 197–211.
Fyfe, W.S., Turner, F.J., and Verhoogen, J. (1958) Metamorphic reactions and metamorphic facies. Geological Society of America Memoir, 85, 215–217.
Harris, P.G. and Brindley, G.W. (1954) Mordenite as an alteration product of a pitchstone glass. American Mineralogist, 39, 819–824.
Hawkins, D.B. (1967) Zeolite studies I. Synthesis of some alkaline earth zeolites. Material Research Bulletin, 2, 951–958.
Hawkins, D.B., Sheppard, R.A., and Gude, A.J. (1978) Hydrothermal synthesis of clinoptilolite and comments on the assemblage phillipsite-clinoptilolite-mordenite. In L.B. Sand and F.A. Mumpton, Eds., Natural Zeolites: Occurrences, Properties, Use, p. 337–343. Pergamon, New York.
Hay, R.L. (1978) Geologic Occurrences of Zeolites. In L.B. Sand, and F.A. Mumpton, Eds., Natural Zeolites: Occurrences, Properties, Use, p. 135–143. Pergamon, New York.
Helgeson, H.C. (1969) Thermodynamics of hydrothermal systems at elevated temperatures and pressures. American Journal of Science, 267, 729–804.
Helgeson, H.C. and Kirkham, D.H. (1974) Theoretical predictions of the thermodynamic behavior of electrolytes at high pressures and temperatures: II. Debye-Hückel parameters for activity coefficients and relative partial-molal properties. American Journal of Science, 274, 1199–1261.
Helgeson, H.C., Delany, J.M., Nesbitt, T.W., and Bird, D.K. (1978) Summary and critique of the thermodynamic properties of rock-forming minerals. American Journal of Science, 278-A, 1–229.
Hemingway, B.S. and Robie, R.A. (1984) Thermodynamic properties of zeolites: low-temperature heat capacities and thermodynamic functions for phillipsite and clinoptilolite. Estimates for the thermochemical properties of zeolitic water at low temperature. American Mineralogist, 69, 692–700.
Hey, R.L. and Bannister, F.A. (1934) Studies on the zeolites. Part VII. "Clinoptilolite", a silica-rich variety of heulandite. Mineralogical Magazine, 23, 556–559.
Iijima, A. (1982) Geology of natural zeolites and zeolitic rocks. In Proceedings of the Fifth International Conference on Zeolites, p. 175–198. Heyden, London.
——(1974) Clay and zeolitic alteration zones surrounding Kuroko deposits in the Hokuroku District, northern Akita, as submarine hydrothermal-diagenetic alteration products. Mining Geology, Special Issue, 6, 267–289.
Ilin, V.G. and Voloshinets, V.G. (1985) Hydrothermal treatment of clinoptilolite and mordenite. In D. Kallo, and H.S. Sherry, Eds., Occurrence, Properties, and Utilization of Natural Zeolites, p. 193–201. Akademiai Press, Budapest.
Johnson J.W., Oelkers E.H., and Helgeson H.C., (1992) Supcrt92: A software package for calculating the standard molal thermodynamic properties of minerals, gases, aqueous species, and reactions from 1 to 5000 bar and 0 °C to 1000 °C. Computers and Geosciences, 18, 899–947.
Johnson, G.K., Tasker, I.R., Jurgens, R., and O'Hare, P.A.G. (1991) Thermodynamic studies of zeolites: clinoptilolite. Journal of Chemical Thermodynamics, 23, 475–484.
Johnson, G.K., Tasker, I.R., Flotow, H.E., and O'Hare, P.A.G. (1992) Thermodynamic studies of mordenite, dehydrated mordenite, and gibbsite. American Mineralogist, 77, 85–93.
Kastenberg, W.E. and Gratton L.J. (1997) Hazards of managing and disposing of nuclear waste. Physics Today, June, 41–47.
Kharaka, Y.K., Gunter, W.D., Aggarwal, P.K., Perkins, E.H., and Debraal, J.D. (1988) SOLMINEQ.88-A computer program for geochemical modelling of water-rock interactions. Water-Resources Investigation Reports, 88–4227, 420 p.
Kieland, J. (1937) Individual activity coefficients of ions in aqueous solutions. Journal of the American Chemical Society, 59, 1675–1679.
Koizumi, M. and Roy, R. (1960) Zeolite studies. I. Synthesis and stability of calcium zeolites. Journal of Geology, 68, 41–53.
Koyama, K. and Takéuchi, Y. (1977) Clinoptilolite: the distribution of potassium atoms and its role in thermal stability. Zeitschrift für Kristallographie, 145, 216–239.
Kusakabe, H., Minato, H., Utada, M., and Yamanaka, T. (1981) Phase relations of clinoptilolite, mordenite, analcime and albite with increasing pH, sodium ion concentration and temperature. Scientific papers of the College of General Education, University of Tokyo, 31(1), 39–59.
Liou, J.G. (1970) Synthesis and stability relations of wairakite, $CaAl_2Si_4O_{12}\cdot 2H_2O$. Contributions to Mineralogy and Petrology, 27, 259–282.
La Iglesia, A. and Aznar, A.J. (1986) A method of estimating the Gibbs energies of formation of zeolites. Zeolites, 6, 26–29.
Mason, B. and Sand, L.B. (1960) Clinoptilolite from Patagonia. The relationship between clinoptilolite and heulandite. American Mineralogist, 45, 341–350.
Mondale, K.D., Mumpton, F.A., and Aplan, F.F. (1988) Properties and benefication of natural sedimentary zeolites. In D.J.T. Carson and A.H. Vassiliou, Eds., Process Mineralogy VIII, p. 249–275. The Minerals, Metals, and Materials Society, Pennsylvania
Mumpton, F.A. (1960) Clinoptilolite redefined. American Mineralogist, 45, 351–369.
——(1978) Natural zeolites: a new industrial mineral commodity. In L.B. Sand, and F.A. Mumpton, Eds., Natural Zeolites: Occurrences, Properties, Use, p. 3–27. Pergamon, New York.
Murphy, W.A., Pabalan, R.T., Prikryl J.D., and Goulet C.J. (1996) Reaction kinetics and thermodynamics of aqueous dissolution and growth of analcime and Na-clinoptilolite at 25 °C. American Journal of Science, 296, 128–196.
Ogard, A.E., Wolfsberg, K., Daniels, W.R., Kerrisk, J., Rundberg, R.S., and Thomas, K.W. (1984) Retardation of radionuclides by rock units along the flow path to the accessible environment. Materials Research Society Symposium Proceedings, 26, 329–336.
Pabalan, R.T. (1994) Thermodynamics of ion exchange between clinoptilolite and aqueous solutions of Na^+/K^+ and Na^+/Ca^{2+}. Geochimica et Cosmochimica Acta, 58, 4573–4590.
Passaglia, E. (1975) The crystal chemistry of mordenite. Contributions to Mineralogy and Petrology, 50, 65–77.
Passaglia, E., Artioli, G., Gualtieri, A., and Carnevali, R. (1995) Diagenetic mordenite from Ponza, Italy. European Journal of Mineralogy, 7, 429–438.
Rimstidt, J.D. and Barnes, H.L. (1980) The kinetics of silica-water reactions. Geochimica et Cosmochimica Acta, 44, 1683–1699.
Sheppard, R.A. (1991) Zeolitic diagenesis of tuffs in the Miocene Chalk Hills Formation, western Snake River Plain, Idaho. U.S. Geological Survey Bulletin, 1963, 27 p. Denver, Colorado.
Smyth, J.R. (1982) Zeolite stability constraints on radioactive waste isolation in zeolite-bearing volcanic rocks. Journal of Geology, 9, 195–201.
Sukheswala, R.N., Avasia, R.K., and Gangopadhyay, M. (1972) Observations on the occurrence of secondary minerals in the Deccan Traps of Western India. Indian Mineralogist, 13, 50–68.
——(1974) Zeolites and associated secondary minerals in the Deccan Traps of Western India. Mineralogical Magazine, 39, 658–671.
Tanger, J.C. and Helgeson, H.C. (1988) Calculation of the thermodynamic and transport properties of aqueous species at high temperatures and pressures: Revised equation of state for the standard partial molal properties of ions and electrolytes. American Journal of Science, 288, 19–98.
Tschernich, R.W. (1992) Zeolites of the World, 563 p. Geoscience Press Inc. Phoenix, Arizona.
Tsitsishvili, G.V, Andronikashvili, T.G., Kirov, G.N., and Filizova, L.D. (1992) Natural Zeolites. In Ellis Horwood, Series in Inorganic Chemistry, 295 p. Ellis Horwood Limited, New York.
Ueda, S., Murata, H., and Koizumi, M. (1980) Crystallization of mordenite from aqueous solutions. American Mineralogist, 65, 1012–1019.
Valueva, G. (1995) Dehydration behavior of heulandite-group zeolites as a function of their chemical composition. European Journal of Mineralogy, 7, 1411–1420.
Walther, J.V. and Helgeson, H.C. (1977) Calculation of the thermodynamic properties of aqueous silica and the solubility of quartz and its polymorphs at high pressures and temperatures. American Journal of Science, 277, 1315–1351.
Wesolowski, D.J. (1992) Aluminum speciation and equilibria in aqueous solution: I. The solubility of gibbsite in the system Na-K-Cl-OH-$Al(OH)_4$ from 0 to 100 °C. Geochimica Cosmochimica Acta, 56, 1065–1091.
Wesolowski, D.J. and Palmer, D.A. (1994) Aluminum speciation and equilibria in aqueous solution: V. Gibbsite solubility at 50 °C and pH 3–9 in 0.1 molal NaCl solutions (a general model for aluminum speciation; analytical methods). Geochimica et Cosmochimica Acta, 58, 2947–2969.
Wilkin, R.T. and Barnes, H.L. (1998a) Solubility and Stability of zeolites in aqueous solution: I. Analcime, Na- and K-clinoptilolite. American Mineralogist, 83, 746–761.
——(1998b) Kinetics of the clinoptilolite to analcime reaction. The Geological Society of America, 1998 Annual Meeting, Abstracts with Program, A-188.
——(1999) Thermodynamics of hydration of Na- and K-clinoptilolite to 300 °C. Physics and Chemistry of Minerals, 26, 468–476.
Wilkin, R.T., Benning, L.G., and Barnes, H.L. (1997) Measurement of zeolite hydration states as functions of T and P_{H_2O}. In D.A. Palmer, and D.J. Wesolowski, Eds., Proceedings of the Fifth International Symposium on Hydrothermal Reactions, p. 88. ORNL, Gatlinburg.
Wirsching, U. (1975) Experimente zum Einflussdes Gesteinsglas-Chemismus auf die Zeolithbildung U. durch hydrothermale Umwandlung. Contribution to Mineralogy and Petrology, 49, 117–124 (in German).
——(1981) Experiments on the hydrothermal formation of calcium zeolites. Clay and Clay Minerals, 29, 171–183.
Zen, E-An (1961) The zeolite facies; an interpretation. American Journal of Science, 259, 401–409.

MANUSCRIPT RECEIVED OCTOBER 13, 1998
MANUSCRIPT ACCEPTED OCTOBER 7, 1999
PAPER HANDLED BY J. WILLIAM CAREY

Appendix on next page

APPENDIX TABLE 1a. Solubility data for clinoptilolite*,† and mordenite†

Sample no.	*T* (°C)	↑↓‡	Time (h)	pH 25 °C	ΣAl (ppm)	ΣSi (ppm)	ΣNa (ppm)	ΣK (ppm)	ΣCa (ppm)	log *K*eq
Na-25-1	25§	↑	2184	6.95	0.21	10.6	11.7	0.11	0.05	–25.94
Na-25-2	25§	↑	2184	6.95	0.23	11.3	6.69	0.11	0.06	–26.03
K-25-1	25§	↑	2184	6.44	0.34	6.18	0.34	5.62	0.06	–27.56
K-25-2	25§	↑	2184	6.44	0.46	7.85	0.35	7.04	0.06	–26.79
Ca-25-1	25§	↑	2184	6.77	0.05	2.91	0.22	0.11	2.59	–28.20
Ca-25-2	25§	↑	2184	6.77	0.11	2.81	0.11	0.11	3.35	–27.88
Wik-25	25§	↑	2184	6.43	0.06	3.17	2.60	0.23	0.06	–16.74
Na-25-1a	25	↑	6840	7.03	1.32	17.1	10.4	0.20	0.01	–24.12
K-25-1a	25	↑	6840	6.60	0.83	9.81	0.21	10.57	0.01	–25.85
K-25-2a	25	↑	6840	6.80	0.73	9.21	0.20	10.16	0.01	–26.06
Ca-25-1a	25	↑	6840	7.58	0.77	3.85	0.05	0.03	3.72	–26.22
Ca-25-2a	25	↑	6840	7.63	0.27	4.70	0.06	0.06	5.71	–26.21
Wik-25a	25	↑	6840	7.18	0.21	6.22	3.41	0.26	0.21	–15.52
Na-25-1b	25	↑	7728	6.62	0.49	13.0	9.24	0.08	0.04	–25.22
Na-25-2b	25	↑	7728	6.71	0.46	13.2	10.10	0.08	0.05	–25.18
K-25-1b	25	↑	7728	6.60	0.69	10.8	1.54	7.56	0.06	–25.90
K-25-2b	25	↑	7728	6.54	0.83	11.0	1.01	7.11	0.05	–25.80
Ca-25-1b	25	↑	7728	6.35	0.27	2.86	1.00	0.04	3.73	–27.35
Ca-25-2b	25	↑	7728	6.34	0.27	3.15	1.19	0.08	5.76	–27.04
Wik-25b	25	↑	7728	6.18	0.13	6.25	4.25	0.30	0.28	–15.62
Na-25-1c	25	↑	8400	7.38	0.57	13.4	8.91	0.09	0.02	–25.10
Na-25-2c	25	↑	8400	7.43	0.85	16.0	9.98	0.07	0.02	–24.49
K-25-1c	25	↑	8400	6.44	0.71	9.4	1.61	5.82	0.02	–26.30
K-25-1c	25	↑	8400	6.44	0.80	10.1	1.9	5.94	0.05	–26.08
Ca-25-1c	25	↑	8400	7.54	0.04	4.4	1.13	0.01	3.33	–27.43
Ca-25-1c	25	↑	8400	7.57	0.04	4.0	0.96	0.01	5.61	–27.27
Wik-25c	25	↑	8400	7.93	0.05	6.1	4.33	0.18	0.24	–15.99
Na-50-1	50§	↑	2184	7.35	0.32	27.6	7.78	0.11	0.05	–23.98
Na-50-2	50§	↑	2184	7.38	0.33	30.0	7.77	0.11	0.06	–23.71
K-50-1	50§	↑	2184	6.72	0.44	20.0	0.22	7.89	0.06	–24.76
K-50-2	50§	↑	2184	6.79	0.43	21.6	0.22	8.12	0.05	–24.59
Ca-50-1	50§	↑	2184	6.84	0.11	7.0	0.33	0.11	3.32	–25.93
Ca-50-2	50§	↑	2184	6.79	0.11	6.5	0.33	0.11	2.96	–26.13
Na-50-2a	50	↑	6840	8.05	1.74	31.8	11.72	0.33	0.01	–22.62
Ca-50-1a	50	↑	6840	7.74	0.30	9.5	0.17	0.19	4.91	–24.69
Ca-50-2a	50	↑	6840	7.66	0.24	9.1	0.17	0.24	4.11	–24.95
Na-50-1b	50	↑	7728	7.10	0.88	35.7	11.9	0.17	0.06	–22.68
Na-50-2b	50	↑	7728	7.00	1.17	38.1	14.0	0.14	0.05	–22.30
K-50-1b	50	↑	7728	6.28	1.25	29.0	1.03	7.25	0.08	–23.51
K-50-2b	50	↑	7728	6.21	1.33	30.6	1.46	10.91	0.07	–23.18
Ca-50-1b	50	↑	7728	6.51	0.13	9.0	1.10	0.11	5.10	–25.20
Ca-50-2b	50	↑	7728	6.55	0.11	10.2	1.51	0.10	5.03	–25.02
Na-50-1c	50	↑	8400	7.95	1.53	34.2	9.44	0.08	0.04	–22.62
Na-50-2c	50	↑	8400	7.92	1.14	32.6	11.61	0.08	0.03	–22.76
K-50-1c	50	↑	8400	7.68	1.44	26.2	1.83	9.29	0.01	–23.55
K-50-2c	50	↑	8400	7.56	1.42	27.1	1.68	9.04	0.03	–23.49
Ca-50-1c	50	↑	8400	7.24	0.16	9.5	0.3	0.1	5.47	–24.99
Ca-50-2c	50	↑	8400	7.38	0.1	9.2	0.29	0.1	4.83	–25.33
c3-0403-1	125	↑	282	8.67	1.39	26.5	1.14	1.01	3.16	–21.90
c3-0403-2	125	↑	282	8.67	1.40	27.9	1.26	0.98	3.35	–21.78
c3-0503-1	125	↑	304	8.72	1.43	30.0	1.30	0.91	3.39	–21.61
c3-0503-2	125	↑	304	8.72	1.32	29.0	1.32	0.92	3.42	–21.72
c3-0603-1	125	↑	328	8.76	1.11	29.6	1.24	0.86	3.46	–21.79
c3-0603-2	125	↑	328	8.76	1.27	28.6	1.43	0.79	3.49	–21.77
c2-2002-1	125	↓	24	6.95	0.27	34.8	0.54	1.20	8.84	–21.89
c2-2002-2	125	↓	24	6.95	0.29	34.4	0.72	1.15	9.02	–21.88
c2-2502-1	125	↓	144	7.02	0.39	31.0	0.77	1.03	7.87	–21.99
c2-2502-2	125	↓	144	7.02	0.37	32.9	0.61	0.97	8.40	–21.87
c3-2703-1	125	↓	39	8.02	0.66	34.1	1.05	0.92	4.85	–21.64
c3-2703-2	125	↓	39	8.02	0.73	34.2	0.98	0.85	5.13	–21.56
c3-3103-1	125	↓	135	7.90	0.96	28.7	1.09	0.68	5.06	–21.80
c3-3103-2	125	↓	135	7.90	1.02	28.1	0.89	0.64	5.37	–21.80
c3-0104-1	125	↓	160	8.05	1.00	26.3	0.88	0.88	5.01	–21.97
c3-0104-2	125	↓	160	8.05	1.03	27.4	0.80	0.91	5.25	–21.86
c2-0602-1	175	↑	62	7.45	1.93	75.8	2.89	1.93	2.21	–19.51
c2-0602-2	175	↑	62	7.45	1.89	78.5	2.84	1.89	2.30	–19.53
c3-0903-1	175	↑	48	8.51	2.02	67.9	2.31	2.17	2.31	–19.81
c3-0903-2	175	↑	48	8.51	1.95	67.6	2.25	2.25	2.25	–19.84
c3-1003-1	175	↑	63	8.53	2.36	72.1	2.36	2.36	2.22	–19.62
c3-1003-2	175	↑	63	8.53	2.27	71.1	2.13	2.56	2.13	–19.68
c3-1103-1	175	↑	89	8.43	1.99	72.9	2.12	1.99	2.38	–19.66
c3-1103-2	175	↑	89	8.43	1.96	71.4	1.96	2.10	2.52	–19.70
c2-1702-1	175	↓	82	7.00	1.36	69.6	3.14	3.55	6.28	–19.72

APPENDIX TABLE 1a.—*Continued*

Sample no.	*T* (°C)	↑↓‡	Time (h)	pH 25 °C	ΣAl (ppm)	ΣSi (ppm)	ΣNa (ppm)	ΣK (ppm)	ΣCa (ppm)	log *K*eq
c2-1702-2	175	↓	82	7.00	1.35	73.0	3.11	3.38	6.76	–19.60
c2-1802-1	175	↓	104	6.95	1.49	67.6	2.30	3.25	6.22	–19.74
c2-1802-2	175	↓	104	6.95	1.54	69.1	2.18	3.20	6.53	–19.67
c3-2303-1	175	↓	70	8.26	2.23	63.4	1.88	2.46	3.29	–19.83
c3-2303-2	175	↓	70	8.26	2.25	62.5	1.88	2.63	3.38	–19.84
c3-2403-1	175	↓	85	8.36	1.83	62.9	2.06	2.17	3.66	–19.91
c3-2403-2	175	↓	85	8.36	1.78	62.8	1.78	2.25	3.79	–19.92
c3-2503-1	175	↓	110	8.29	2.27	60.6	1.89	2.14	3.66	–19.89
c3-2503-2	175	↓	110	8.29	2.34	59.8	1.87	2.23	3.75	–19.89
c1-2501-1	225	↑	24	7.36	0.82	207	2.60	3.25	1.95	–17.93
c1-2501-2	225	↑	24	7.36	0.79	194	2.24	3.28	1.94	–18.09
c1-2601-1	225	↑	48	7.49	0.82	200	2.83	3.37	1.75	–18.03
c1-2701-1	225	↑	72	7.44	0.86	183	2.69	1.88	2.29	–18.13
c1-2701-2	225	↑	72	7.44	0.90	189	2.87	1.69	2.48	–18.02
c2-0802-1	225	↑	42	7.09	2.45	166	3.95	2.86	1.77	–17.89
c2-0802-2	225	↑	42	7.09	2.39	166	3.85	2.92	1.86	–17.90
c2-0902-1	225	↑	67.5	6.95	2.25	160	3.71	1.06	1.59	–18.03
c2-0902-2	225	↑	67.5	6.95	2.26	165	3.73	3.59	1.60	–17.97
c3-1303-1	225	↑	43	7.97	2.52	150	2.65	2.52	1.19	–18.20
c3-1303-2	225	↑	43	7.97	2.50	153	2.64	2.64	1.17	–18.16
c3-1403-1	225	↑	67	7.98	2.58	151	2.71	2.85	0.95	–18.23
c3-1403-2	225	↑	67	7.98	2.62	150	2.62	2.91	1.02	–18.22
c3-1503-2	225	↑	95	7.92	2.62	143	2.49	2.86	1.12	–18.29
c2-1302-1	225	↓	59	7.54	1.91	141	3.31	4.58	2.16	–18.31
c2-1302-2	225	↓	59	7.54	1.92	143	3.30	4.53	2.20	–18.28
c3-1903-2	225	↓	46	7.63	2.58	140	2.58	3.64	0.94	–18.39
c3-2003-1	225	↓	70	7.63	2.64	138	2.52	3.40	1.01	–18.38
c3-2003-2	225	↓	70	7.63	2.70	138	2.56	3.64	1.08	–18.36
c1-2801-3	265	↑	24	7.09	1.65	259	3.98	1.65	1.65	–17.17
c1-2801-4	265	↑	24	7.09	1.75	269	3.91	1.48	1.75	–17.04
c3-1503-3	265	↑	2	7.35	3.50	204	2.55	3.02	0.64	–17.55
c3-1503-4	265	↑	2	7.35	3.62	208	2.41	2.68	0.80	–17.44
c3-1603-1	265	↑	17	7.46	3.13	218	2.61	2.87	0.52	–17.51
c3-1603-2	265	↑	17	7.46	3.15	221	2.43	2.86	0.57	–17.44
c3-1603-3	265	↑	26	7.34	3.05	229	2.52	2.92	0.40	–17.48
c3-1603-4	265	↑	26	7.34	3.02	229	2.61	3.02	0.41	–17.48
c2-1002-3	265	↓	24	6.18	2.23	263	3.80	3.80	0.82	–17.15
c2-1002-4	265	↓	24	6.18	2.41	269	3.93	3.81	0.84	–17.06
c2-1002-1	275	↑	12	6.09	2.48	272	3.60	3.48	1.08	–16.96
c2-1002-2	275	↑	12	6.09	2.46	275	3.37	3.37	1.08	–16.95

* Samples coded as Na-x, K-x, Wik-x, are Na-, and Cpt-K and Wikiup analcime; all others are Cpt-Ca.
† In all charge balance calculations the total positive charge was balanced by $Al(OH)_4^-$ and Cl^-.
‡ Direction of approach to saturation.
§ Data not used for the averages tabulated in Table 2 (see text).

APPENDIX TABLE 1b. Solubility data for Mor-Cadenite

Sample no.	*T* (°C)	↑↓	time (h)	pH 25 °C	Al (ppm)	Si (ppm)	Na (ppm)	K (ppm)	Ca (ppm)	log*K*eq
M-25-1	25*	↑	3480	8.43	0.17	8.54	1.01	0.04	3.86	–25.28
M-25.2	25*	↑	3480	8.81	0.18	8.65	0.96	0.04	3.92	–25.21
M-25-3	25*	↑	4200	9.1	0.14	8.64	0.99	0.01	4.96	–25.27
M-25-4	25*	↑	4200	9.3	0.15	7.73	0.46	0.01	4.38	–25.50
m1-1404-1	100	↑	259	7.93	1.33	20	0.27	0.13	4.67	–22.14
m1-1404-2	100	↑	259	7.93	1.08	19	0.13	0.07	4.72	–22.36
m1-1504-1	100	↑	283	8.03	1.38	21	0.41	0.28	4.56	–22.06
m1-1504-2	100	↑	283	8.03	1.07	19	0.12	0.06	4.65	–22.34
m1-1604-1	100	↑	309	8.04	1.17	19	0.26	0.13	4.41	–22.28
m1-1604-2	100	↑	309	8.04	1.03	19	0.13	0.06	4.78	–22.32
m2-1206-1	100	↑	336	8.83	1.13	20	0.14	0.14	4.53	–22.24
m2-1206-2	100	↑	336	8.83	1.06	21	0.07	0.07	5.04	–22.10
m2-1506-1	100	↑	417	8.77	0.83	14	0.17	0.08	3.16	–22.15
m2-1506-2	100	↑	417	8.77	1.19	21	0.13	0.07	4.77	–22.06
m2-1906-1	100	↑	504	7.72	1.08	20	0.12	0.12	4.33	–22.21
m2-1906-2	100	↑	504	7.72	1.09	21	0.06	0.06	4.48	–22.18
m2-2707-1	100	↓	194	7.96	1.04	17	0.13	0.06	3.77	–22.67
m2-2707-2	100	↓	194	7.96	1.22	18	0.06	0.06	3.87	–22.49
m2-2807-1	100	↓	212	7.96	1.28	17	0.26	0.06	3.70	–22.62
m2-2807-2	100	↓	212	7.96	1.24	16	0.06	0.06	3.73	–22.68

APPENDIX TABLE 1b.—*Continued*

Sample no.	*T* (°C)	↑↓	time (h)	pH 25 °C	Al (ppm)	Si (ppm)	Na (ppm)	K (ppm)	Ca (ppm)	log*K*eq
m2-1607-1	125	↓	63	7.79	1.07	37	0.27	0.13	3.20	–20.98
m2-1607-2	125	↓	63	7.79	1.03	36	0.13	0.06	3.21	–21.08
m2-1907-1	125	↓	133	7.97	1.54	24	0.13	0.06	3.71	–21.71
m2-1907-2	125	↓	133	7.97	1.56	25	0.07	0.07	3.91	–21.65
m2a-1808-1	130	↓	96	7.85	1.92	27	3.16	0.07	4.53	–21.30
m2a-1808-2	130	↓	96	7.85	2.02	28	1.12	0.06	4.60	–21.23
m1-2004-1	150	↑	69	8.12	2.16	37	0.38	0.13	5.72	–20.56
m1-2004-2	150	↑	69	8.12	2.19	39	0.34	0.08	6.07	–20.43
m1-2104-1	150	↑	92	8.06	2.04	37	0.36	0.12	5.52	–20.57
m1-2104-2	150	↑	92	8.06	2.14	40	0.15	0.08	6.26	–20.39
m1-2304-1	150	↑	142	7.90	2.09	39	0.26	0.13	5.89	–20.43
m1-2304-2	150	↑	142	7.90	2.21	40	0.13	0.07	6.24	–20.34
m2-2206-1	150	↑	71	8.30	1.62	47	0.44	0.15	4.56	–20.21
m2-2206-2	150	↑	71	8.30	1.68	48	0.36	0.06	4.93	–20.13
m2-2406-1	150	↑	118	8.33	1.60	49	0.37	0.12	4.55	–20.13
m2-2406-2	150	↑	118	8.33	1.71	50	0.23	0.06	4.91	–20.03
m1-2604-1	175	↑	65	7.83	2.09	54	0.97	0.14	5.84	–19.74
m1-2604-2	175	↑	65	7.83	2.16	59	0.86	0.14	6.18	–19.53
m1-2804-1	175	↑	116	7.86	2.15	57	1.00	0.14	6.30	–19.59
m1-2804-2	175	↑	116	7.86	2.16	58	0.86	0.14	6.48	–19.57
m1-2904-1	175	↑	131	7.95	2.31	60	0.81	0.12	6.58	–19.45
m1-2904-2	175	↑	131	7.95	2.35	60	0.91	0.13	6.78	–19.44
m2-2806-1	175	↑	74	8.08	1.93	75	0.84	0.12	3.86	–19.17
m2-2806-2	175	↑	74	8.08	2.00	75	0.80	0.13	4.53	–19.12
m2a-0208-1	175	↑	119	7.85	2.55	65	0.67	0.06	4.77	–19.29
m2a-0208-2	175	↑	119	7.85	2.59	65	0.65	0.08	5.01	–19.30
m2-0107-1	200	↑	72	7.86	2.03	96	1.27	0.13	3.30	–18.63
m2-0107-2	200	↑	72	7.86	2.02	102	1.13	0.13	3.65	–18.49
m2-0207-1	200	↑	96	7.78	2.00	103	1.28	0.29	3.14	–18.52
m2-0207-2	200	↑	96	7.78	2.01	104	1.13	0.13	3.39	–18.47
m2-1107-1	200	↓	44	7.80	2.29	97	0.64	0.13	3.95	–18.54
m2-1107-2	200	↓	44	7.80	2.15	95	0.40	0.13	3.90	–18.59
m2-1307-1	200	↓	70	7.74	2.13	96	0.50	0.13	3.88	–18.58
m2-1307-2	200	↓	70	7.74	2.30	98	0.61	0.15	3.83	–18.51
m2-0607-1	225	↑	95	7.75	2.15	130	1.56	0.36	2.75	–18.00
m2-0607-2	225	↑	95	7.75	2.18	131	1.24	0.16	2.64	–18.00
m2-0707-1	225	↑	117	7.67	2.40	126	1.42	0.22	2.83	–18.01
m2-0707-2	225	↑	117	7.67	2.41	126	1.42	0.14	2.98	–18.00
m2a-0708-1	225	↑	117	7.65	2.33	118	0.78	0.13	3.49	–18.13
m2a-0708-2	225	↑	117	7.65	2.30	118	0.54	0.14	3.38	–18.15
m2a-1108-1	225	↓	80	7.54	2.21	114	0.47	0.02	3.64	–18.22
m2a-1108-2	225	↓	80	7.54	2.27	116	0.36	0.01	3.71	–18.16
m1-0105-2	250	↑	41	8.10	4.46	100	2.68	0.15	5.50	–18.10
m1-0505-5	250	↑	149	7.65	2.23	138	2.23	0.30	2.68	–18.46
m1-0505-6	250	↑	149	7.65	2.33	146	2.07	0.26	3.11	–18.38
m2-0807-1	250	↑	22	7.54	2.37	157	1.75	0.25	2.12	–17.61
m2-0807-2	250	↑	22	7.54	2.32	158	1.59	0.24	2.20	–17.61
m2-0907-1	250	↑	44	7.54	2.17	159	1.45	0.24	2.17	–17.62
m2-0907-2	250	↑	44	7.54	2.22	156	1.37	0.17	2.05	–17.67
m2a-0808-1	260	↑	24	7.48	2.23	154	0.59	0.15	2.82	–17.61
m2a-0808-1	260	↑	24	7.48	2.21	159	0.44	0.15	2.81	–17.55
m1-0605-3	265	↑	22	7.68	1.99	156	1.46	0.27	1.33	–17.81
m1-0605-4	265	↑	22	7.68	2.14	166	1.53	0.15	1.53	–17.61

* Data not used for fit in Equation 7.
† In all charge balance calculations the total positive charge was balanced by $Al(OH)_4^-$ and Cl^-.
‡ Direction of approach to saturation.

APPENDIX TABLE 2. Ionization constants and sources

Equilibria/	Log *K*												
T °C	25°	50°	100°	125°	150°	175°	200°	225°	250°	260°	265°	275°	ref.
(1)	–13.99	–13.27	–12.27	–11.92	–11.64	–11.43	–11.28	–11.19	–11.18	–11.19	–11.21	–11.25	(a)
(2)	–16.12	–13.92	–10.47	–9.10	–7.90	–6.85	–5.93	–5.11	–4.38	–4.11	–3.98	–3.73	(b)
(3)	–22.16	–19.97	–16.40	–14.93	–13.62	–12.44	–11.37	–10.39	–9.50	–9.17	–9.00	–8.68	(b)
(4)	–9.82	–9.50	–9.10	–8.98	–8.90	–8.85	–8.85	–8.89	–8.96	–9.02	–9.04	–9.07	(c)

Notes: (a) Marshal and Frank (1981); (b) Bourcier et al. (1993); (c) Busey and Messmer (1977).
(1) $H_2O_l \leftrightarrow H+ + OH^-$; (2) $Al^{3+} + 3H_2O = Al(OH)_3^0 + 3H^+$; (3) $Al^{3+} + 4H_2O = Al(OH)_4^- + 4H^+$; (4) $H_4SiO_4 = H_3SiO_4^- + H^+$.